

UC San Diego

UC San Diego Previously Published Works

Title

Fluorescence-guided surgery of retroperitoneal-implanted human fibrosarcoma in nude mice delays or eliminates tumor recurrence and increases survival compared to bright-light surgery.

Permalink

<https://escholarship.org/uc/item/16g4p47c>

Journal

PloS one, 10(2)

ISSN

1932-6203

Authors

Uehara, Fuminari
Hiroshima, Yukihiro
Miwa, Shinji
et al.

Publication Date

2015

DOI

10.1371/journal.pone.0116865

Peer reviewed

RESEARCH ARTICLE

Fluorescence-Guided Surgery of Retroperitoneal-Implanted Human Fibrosarcoma in Nude Mice Delays or Eliminates Tumor Recurrence and Increases Survival Compared to Bright-Light Surgery

Fuminari Uehara^{1,2,3}, Yukihiro Hiroshima^{1,2}, Shinji Miwa^{1,2}, Yasunori Tome^{1,2,3}, Shuya Yano^{1,2}, Mako Yamamoto¹, Yasunori Matsumoto², Hiroki Maehara³, Kazuhiro Tanaka³, Michael Bouvet², Fuminori Kanaya³, Robert M. Hoffman^{1,2*}

1 AntiCancer, Inc., 7917 Ostrow Street, San Diego, California 92111, United States of America, **2** Department of Surgery, University of California San Diego, 200 West Arbor Drive, San Diego, California 92103, United States of America, **3** Department of Orthopedic Surgery, Graduate School of Medicine, University of the Ryukyus, 207 Uehara, Nishihara, Okinawa 903-0125, Japan

* all@anticancer.com



OPEN ACCESS

Citation: Uehara F, Hiroshima Y, Miwa S, Tome Y, Yano S, Yamamoto M, et al. (2015) Fluorescence-Guided Surgery of Retroperitoneal-Implanted Human Fibrosarcoma in Nude Mice Delays or Eliminates Tumor Recurrence and Increases Survival Compared to Bright-Light Surgery. PLoS ONE 10(2): e0116865. doi:10.1371/journal.pone.0116865

Academic Editor: Shree Ram Singh, National Cancer Institute, UNITED STATES

Received: October 10, 2014

Accepted: December 15, 2014

Published: February 24, 2015

Copyright: © 2015 Uehara et al. This is an open access article distributed under the terms of the [Creative Commons Attribution License](https://creativecommons.org/licenses/by/4.0/), which permits unrestricted use, distribution, and reproduction in any medium, provided the original author and source are credited.

Data Availability Statement: Please note that all raw data necessary to replicate the findings and conclusions in our study are freely available in the paper.

Funding: This study was supported by the National Cancer Institute grant CA142669. The funder had no role in study design, data collection and analysis, decision to publish, or preparation of the manuscript.

Competing Interests: Yukihiro Hiroshima, Shinji Miwa, Shuya Yano, Mako Yamamoto, and Robert M. Hoffman are unpaid affiliates of AntiCancer Inc.

Abstract

The aim of this study is to determine if fluorescence-guided surgery (FGS) can eradicate human fibrosarcoma growing in the retroperitoneum of nude mice. One week after retroperitoneal implantation of human HT1080 fibrosarcoma cells, expressing green fluorescent protein (GFP) (HT-1080-GFP), in nude mice, bright-light surgery (BLS) was performed on all tumor-bearing mice ($n = 22$). After BLS, mice were randomized into 2 treatment groups; BLS-only ($n = 11$) or the combination of BLS + FGS ($n = 11$). The residual tumors remaining after BLS were resected with FGS using a hand-held portable imaging system under fluorescence navigation. The average residual tumor area after BLS + FGS was significantly smaller than after BLS-only ($0.4 \pm 0.4 \text{ mm}^2$ and $10.5 \pm 2.4 \text{ mm}^2$, respectively; $p = 0.006$). Five weeks after surgery, the fluorescent-tumor areas of BLS- and BLS + FGS-treated mice were $379 \pm 147 \text{ mm}^2$ and $11.7 \pm 6.9 \text{ mm}^2$, respectively, indicating that FGS greatly inhibited tumor recurrence compared to BLS. The combination of BLS + FGS significantly decreased fibrosarcoma recurrence compared to BLS-only treated mice ($p < 0.001$). Mice treated with BLS+FGS had a significantly higher disease-free survival rate than mice treated with BLS-only at five weeks after surgery. These results suggest that combination of BLS + FGS significantly reduced the residual fibrosarcoma volume after BLS and improved disease-free survival.

Introduction

Most tumors in the retroperitoneum are malignant, and about one third of these are soft tissue sarcomas [1, 2]. Retroperitoneal tumors present several therapeutic challenges because of their

Fuminari Uehara and Yasunori Tome were former affiliates of AntiCancer Inc. Robert M. Hoffman is a PLOS ONE Editorial Board Member. AntiCancer Inc. markets animal models of cancer. There are no other competing interests. There are no patents, products in development, or marketed products to declare. This does not alter the authors' adherence to all the PLOS ONE policies on sharing data and materials.

relative late presentation and anatomical location [3]. Complete tumor resection can potentially be a curative treatment modality for retroperitoneal soft tissue sarcoma patients [4], but local recurrence occurs in a large proportion of patients and is responsible for as many as 75% of sarcoma-related deaths [5].

Local recurrence often occurs following attempted curative resection of the primary tumor, because all cancer cells are not removed by the surgeon due to the inability to see them. Making tumors fluorescence offers great advantages for fluorescence-guided surgery (FGS) to achieve complete resection [6].

Our laboratory has developed FGS of cancer using both fluorescent-protein labeling of the tumor [7–16] as well as fluorescent-antibody labeling of the tumor [17–29], in orthotopic nude mouse models of human tumors, including patient-derived orthotopic (PDOX) models [24, 25, 30].

In the present study, we report the effectiveness of using FGS to improve outcomes in a retroperitoneal-implanted nude-mouse model of human fibrosarcoma, including reducing residual tumor tissue, thereby decreasing tumor recurrence and increasing disease-free survival.

Materials and Methods

Ethics Statement

All animal studies were conducted with an AntiCancer Institutional Animal Care and Use Committee (IACUC)-protocol specifically approved for this study and in accordance with the principals and procedures outlined in the National Institute of Health Guide for the Care and Use of Animals under Assurance Number A3873-1. In order to minimize any suffering of the animals the use of anesthesia and analgesics were used for all surgical experiments. Animals were anesthetized with a 20 μ L mixture of ketamine (20 mg/kg), acepromazine (0.48 mg/kg), and xylazine (15.2 mg/kg) by intramuscular injection 10 minutes before surgery. The response of animals during surgery was monitored to ensure adequate depth of anesthesia. Ibuprofen (7.5 mg/kg orally in drinking water every 24 hours for 7 days post-surgery) was used in order to provide analgesia post-operatively in the surgically-treated animals. The animals were observed on a daily basis and humanely sacrificed by CO₂ inhalation when they met the following humane endpoint criteria: prostration, skin lesions, significant body weight loss, difficulty breathing, epistaxis, rotational motion and body temperature drop. The use of animals was necessary to understand the *in vivo* efficacy, in particular, anti-metastatic efficacy of the procedures tested. Animals were housed with no more than 5 per cage. Animals were housed in a barrier facility on a high efficiency particulate air (HEPA)-filtered rack under standard conditions of 12-hour light/dark cycles. The animals were fed an autoclaved laboratory rodent diet (S1 ARRIVE Checklist).

Establishment of a green fluorescent protein labeled HT-1080 fibrosarcoma cell line

For green fluorescent protein (GFP) gene transduction of human HT-1080 fibrosarcoma cells [31, 32], 80% confluent cells were used. Briefly, cells were incubated with a 1:1 precipitated mixture of retroviral supernatants, of packaging PT67-GFP cells [33–35], which express the GFP gene linked to the G418 resistance gene (Clontech, Mountain View, CA) and RPMI 1640 medium (Cellgro, Herndon, VA, USA) containing 10% fetal bovine serum (FBS) (Omega Scientific, San Diego, CA, USA) for 72 h. Fresh medium was replenished at this time. Cells were harvested with trypsin/EDTA 72 h post-transduction and subcultured at a ratio of 1:15 into medium, which contained 200 μ g/ml of the selective agent G418. The level of G418 was increased stepwise up to 800 μ g/ml [33–35].

Cell culture

HT1080-GFP cells were maintained in RPMI 1640 medium supplemented with 10% FBS and 1% penicillin/streptomycin. The cells were incubated at 37°C in a humidified atmosphere of 5% CO₂ in air and harvested by trypsinization at 80% confluence.

Mice

Athymic nu/nu nude mice (AntiCancer Inc., San Diego, CA) were used in this study. Mice were kept in a barrier facility under HEPA filtration. Mice were fed with an autoclaved laboratory rodent diet. All mouse surgical procedures and imaging were performed with the animals anesthetized by subcutaneous injection of the ketamine mixture described above (20 µl).

All animal studies were conducted with an AntiCancer Institutional Animal Care and Use Committee (IACUC)-protocol specifically approved for this study and in accordance with the principals and procedures outlined in the National Institute of Health Guide for the Care and Use of Animals under Assurance Number A3873-1.

Retroperitoneal implantation of HT1080-GFP cells

Four-week-old female nude mice were anesthetized by the ketamine mixture via s.c. injection. The back was sterilized with alcohol. An approximately 1 cm skin incision was made just to the right side of spine in order to expose the retroperitoneum. HT1080-GFP cells (1×10^6) in Matrigel (5 µl) (BD Bioscience, San Jose, CA) per mouse were injected into the retroperitoneum with a 0.5 ml 28 G latex-free insulin syringe (TYCO Health Group LP, Mansfield, MA). The skin was closed with a 6-0 suture.

Fluorescence imaging

The Olympus OV100 Small Animal Imaging System (Olympus Corp., Tokyo, Japan), containing an MT-20 light source (Olympus Biosystems, Planegg, Germany) and DP70 CCD camera (Olympus Corp., Tokyo, Japan) [36]; the Dino-Lite imaging system (AM4113T-GFBW Dino-Lite Premier; AnMo Electronics Corporation, Taiwan) [30]; and the MVX10 long-working distance microscope (Olympus Corp.) [37] were used for imaging live mice. To analyze for recurrence and to follow tumor progression postoperatively, weekly noninvasive whole-body imaging of the mice was performed using the iBox Scientia Small Animal Imaging System (UVP LLC, Upland, CA, USA). GFP fluorescent-tumor areas were recorded every week [16, 38–40]. The working-distance setting for GFP imaging in the iBox was adjusted to image the maximum possible fluorescent area in each mouse both before surgery and after surgery. All images were analyzed with ImageJ v1.440 (National Institutes of Health).

Tumor resection

One week after retroperitoneal implantation of HT1080-GFP cells, bright-light surgery (BLS) was performed to all tumor-bearing mice ($n = 22$). The exposed retroperitoneal tumor was imaged preoperatively with the OV100 at a magnification of 0.14×. Resection of the primary tumor was performed under standard bright-field using the MVX10 microscope [37]. For fibrosarcoma resection, intralesional and marginal tumor excision was performed in all the mice. Postoperatively, the surgical resection bed was imaged with the OV100 at a magnification of 0.14× or 0.56× to detect residual tumor. The mice which underwent BLS were randomized into 2 treatment groups: BLS only ($n = 11$) and BLS + FGS ($n = 11$) (Fig. 1). The residual tumors of the BLS + FGS group of mice were resected using the Dino-Lite imaging system under fluorescence navigation. After completion of FGS, the surgical resection bed was imaged with the OV100 at a

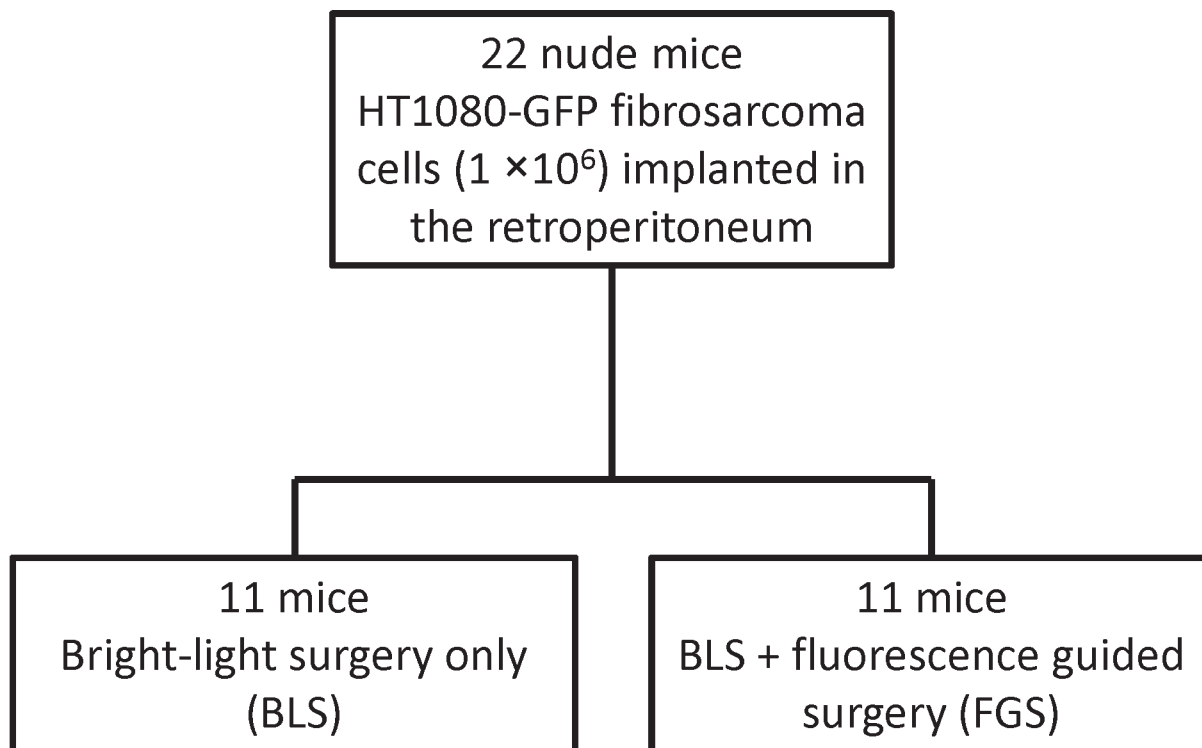


Figure 1. Schematic diagram of the experimental protocol. One week after retroperitoneal fibrosarcoma implantation in 22 mice, the tumor-bearing mice were randomly assigned to either the BLS-only or BLS + FGS groups. Resection of the tumor was performed using the Dino-Lite imaging system under fluorescence navigation (14). Postoperatively, the surgical resection bed was imaged with the OV100 at a magnification of 0.14× or 0.56× to detect residual fibrosarcoma cells.

doi:10.1371/journal.pone.0116865.g001

magnification of 0.14× or 0.89× to detect microscopic minimal residual cancer (MRC) [41]. The incision was closed in one layer using 6-0 nylon surgical sutures after treatment.

Statistical analysis

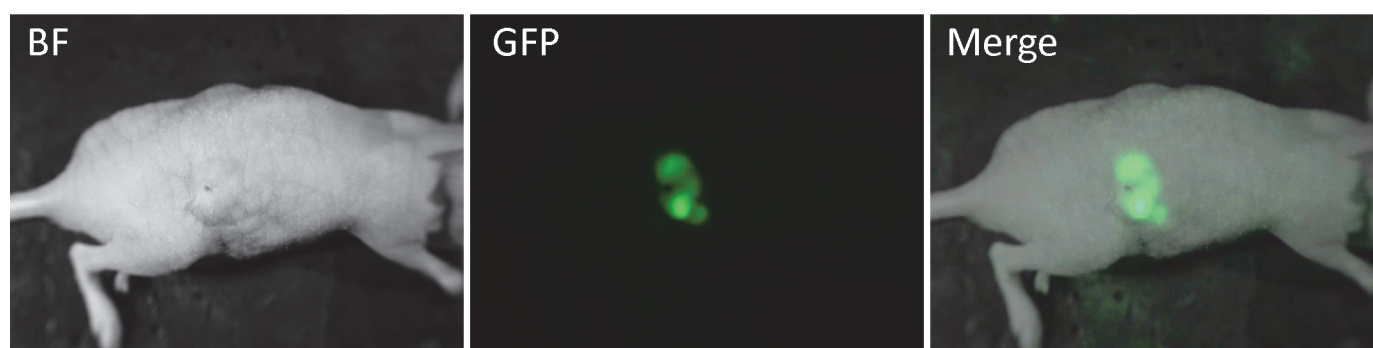
Statistical analyses were performed with EZR (Saitama Medical Center, Jichi Medical University). Residual tumor area is expressed as mean ± SD. The two-tailed Student's t-test was used to compare continuous variables between 2 groups. Kaplan-Meier survival curves were used for demonstrating mouse survival. Survival outcomes were compared using log rank tests. A p value < 0.05 was considered statistically significant.

Results and Discussion

Efficacy of bright-light and bright-light plus fluorescence-guided surgery

Retroperitoneal mouse models of HT-1080-GFP human fibrosarcoma were established in 22 mice (Fig. 2A). One week after retroperitoneal implantation, the mice were randomly divided into the BLS or BLS + FGS groups (11 mice in each group) (Fig. 1). Before surgical resection, the fluorescent-tumor areas of the mice in the BLS and BLS + FGS groups were $41.3 \pm 15.4 \text{ mm}^2$ and $47.9 \pm 30.6 \text{ mm}^2$, respectively (Fig. 2B). There was no significant difference in pre-operative tumor burden between BLS and BLS + FGS mice. A great improvement in visualization of the primary fibrosarcoma during FGS enhanced distinction of tumor from surrounding soft tissues and identified a larger extent of tumor growth due to GFP expression by the tumor (Fig. 3A). FGS following BLS resulted in a more complete resection of the fibrosarcoma,

A



B

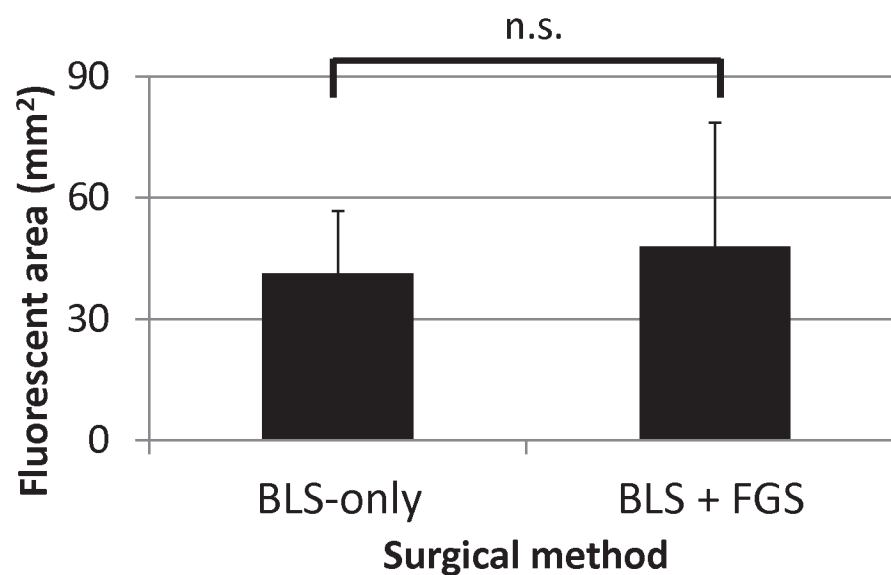


Figure 2. Pre-operative images of retroperitoneal fibrosarcoma mouse model. A. Retroperitoneal fibrosarcoma mouse model. B. Fluorescent-tumor areas before surgery. There was no significant difference in fluorescent-tumor areas between the BLS-only and BLS + FGS mouse groups. The fluorescent areas of tumors are expressed mean \pm SD. All residual tumors expressing GFP were imaged with the Olympus OV100 Small Animal Imaging System (Olympus Corp.) [36] and analyzed with ImageJ v1.440 (National Institutes of Health). Statistical analysis was performed using the Student's t-test.

doi:10.1371/journal.pone.0116865.g002

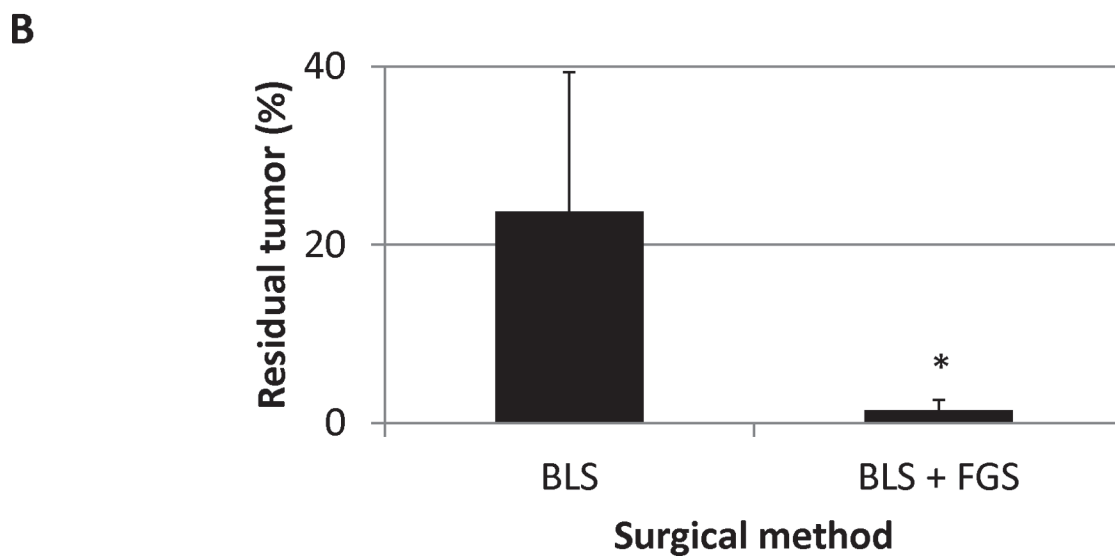
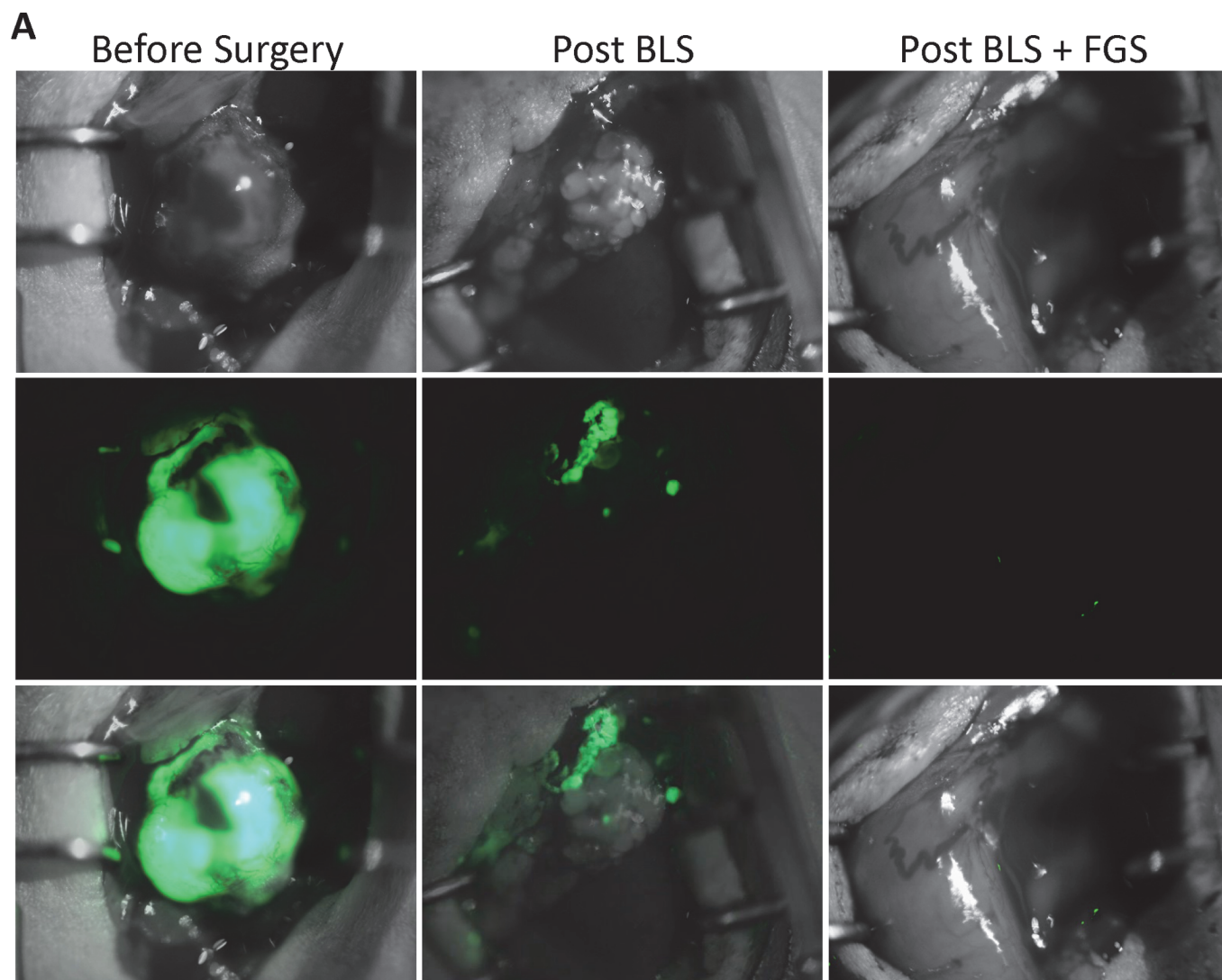


Figure 3. Pre-operative and post-operative images of retroperitoneal fibrosarcoma. A. Pre- and post-operative images of mice in the BLS-only and BLS + FGS groups. Upper panels are bright-field (BF), middle panels show GFP tumor fluorescence, and lower panels show merged images. The residual tumor after BLS-only was clearly detected with the OV100 at a magnification of 0.56x. The residual tumor after BLS + FGS was marginally detected with the OV100. Fluorescent area of residual tumor after BLS-only and BLS + FGS. Fluorescent areas of residual tumors in BLS-only and BLS + FGS group were $10.5 \pm 2.4 \text{ mm}^2$ and $0.4 \pm 0.4 \text{ mm}^2$, respectively. The residual tumor area after BLS + FGS was significantly smaller than after BLS-only. All images were measured for residual tumor areas using ImageJ. * $p < 0.01$. B. Bar graphs show the percent of the original tumor remaining after either BLS or the combination of BLS + FGS.

doi:10.1371/journal.pone.0116865.g003

demonstrated by a significant decrease in the fluorescent area of the residual tumor compared to BLS-only. Fluorescent areas of the residual tumors after BLS and the combination of BLS + FGS were $10.5 \pm 2.4 \text{ mm}^2$ and $0.4 \pm 0.4 \text{ mm}^2$, respectively (Fig. 3B; $p = 0.00597$).

Time-course imaging of recurrent tumor growth after BLS or the combination of BLS + FGS

Time-lapse imaging visualized rapid growth of the fluorescent area in the BLS-only-treated mice after surgery (Fig. 4). Fluorescent-tumor areas of the mice treated with BLS-only rapidly increased, whereas mice treated with BLS + FGS had minimal tumor recurrence (Fig. 5). Five weeks after surgery, the fluorescent areas of BLS-only- and BLS + FGS-treated mice were $379 \pm$

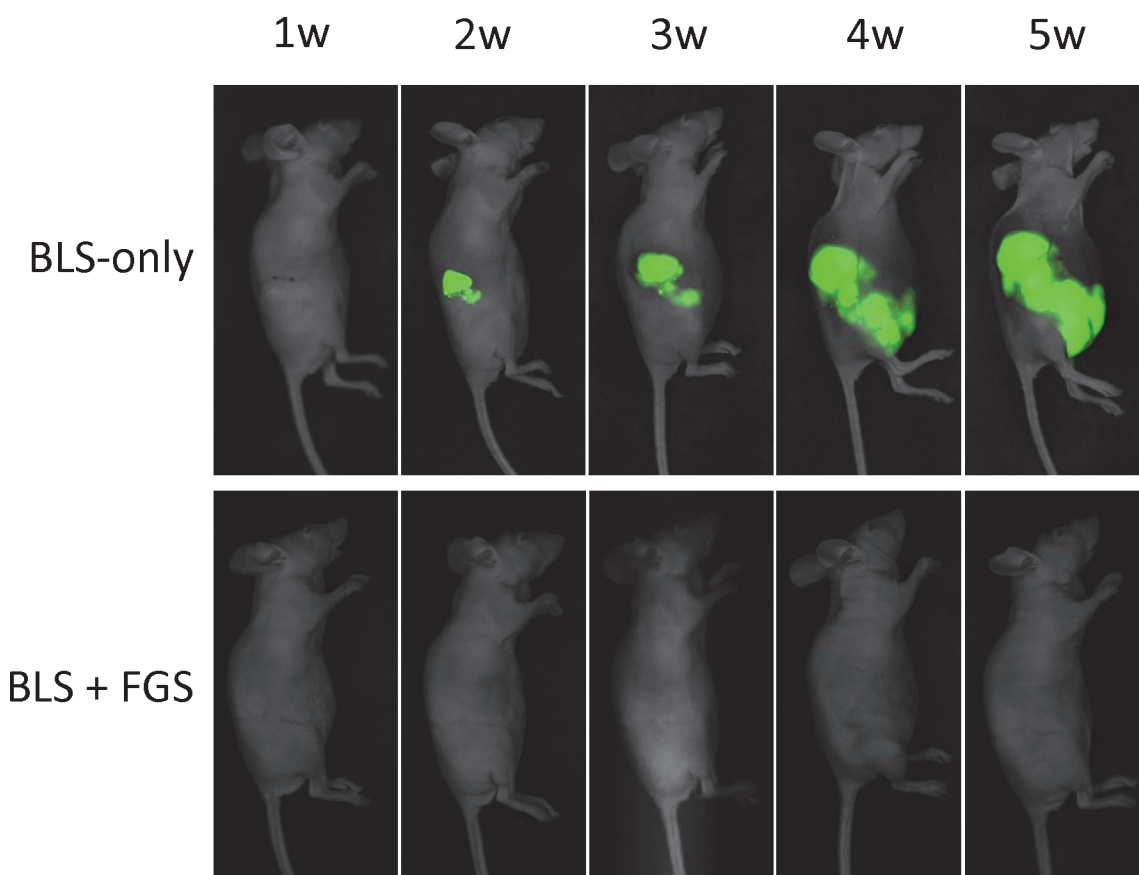


Figure 4. Representative time-course imaging of tumor recurrence after BLS-only and the combination of BLS + FGS. Fluorescence imaging, using the iBOX Scientia Small Animal Imaging System [34, 52, 53], showed BLS-only mice treated had tumor recurrence. In contrast, mice treated with the combination of BLS + FGS showed little recurrent tumor growth.

doi:10.1371/journal.pone.0116865.g004

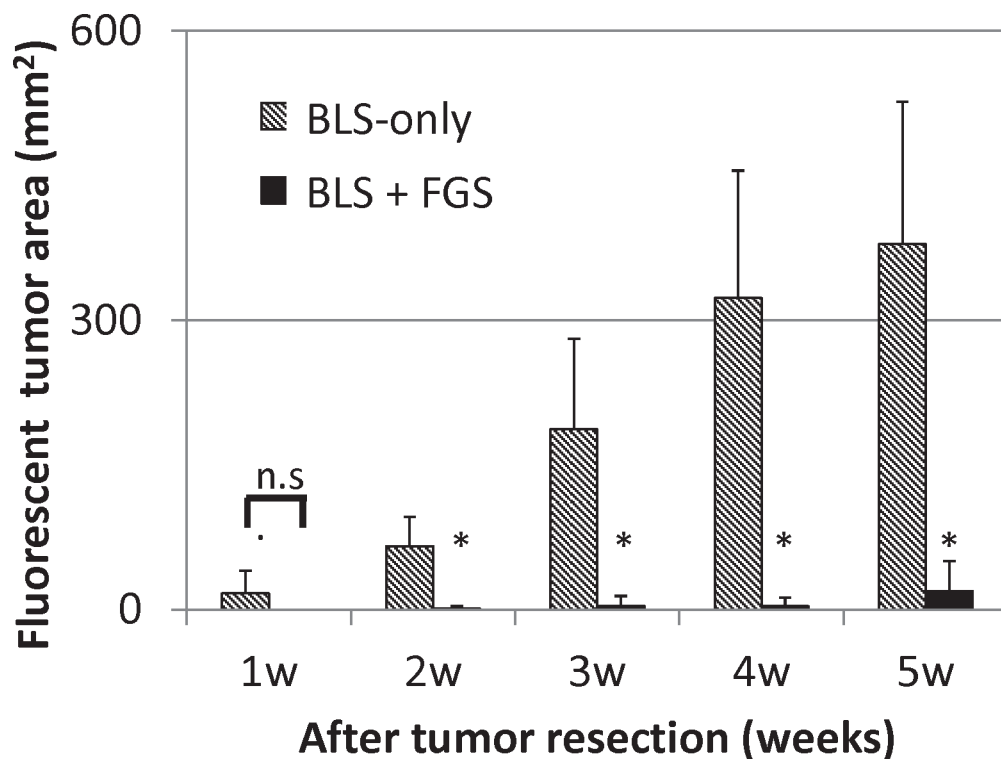


Figure 5. Extent of tumor recurrence after BLS-only or BLS+FGS. BLS-only treated mice had tumor recurrence. BLS + FGS-treated mice had only minimal growth of recurrent tumors. Five weeks after surgery, the fluorescent-tumor areas of BLS-only- and BLS+FGS-treated mice were $379 \pm 147 \text{ mm}^2$ and $11.7 \pm 6.9 \text{ mm}^2$, respectively. The combination of BLS + FGS significantly decreased recurrence compared to BLS-only treated mice. * $p < 0.001$.

doi:10.1371/journal.pone.0116865.g005

147 mm^2 and $11.7 \pm 6.9 \text{ mm}^2$, respectively (Fig. 5). The combination of BLS+FGS significantly decreased tumor recurrent more than BLS-only treated mice ($p < 0.001$).

Disease-free survival (DFS) after BLS and BLS + FGS

Five-week DFS rates of BLS-only- and BLS + FGS-treated mice were 9.1% and 81.8%, respectively (Fig. 6). Mice treated with BLS + FGS had a significantly higher survival rate than mice treated with BLS-only ($p < 0.005$). These results further suggest that FGS significantly reduced the residual tumor volume after BLS and improved DFS.

We have previously demonstrated the enhanced visualization and resection of primary and metastatic cancer labeled with GFP [7–16] or fluorescent antibodies [17–29]. The results of these previous studies show the great potential of FGS. The present study demonstrates that FGS can be beneficial for patients with retroperitoneal sarcoma to prevent recurrence of the tumor, a major current problem in the clinic. A possible translatable method to label the fibrosarcoma in the clinic could be with a GFP-containing, telomerase-dependence adenovirus which effectively and selectively labels tumors in mouse models, enabling FGS [7–9]. Another possibility could be the use of RNA-guided nano-sensors to specifically label cancer cells in vivo for FGS [42].

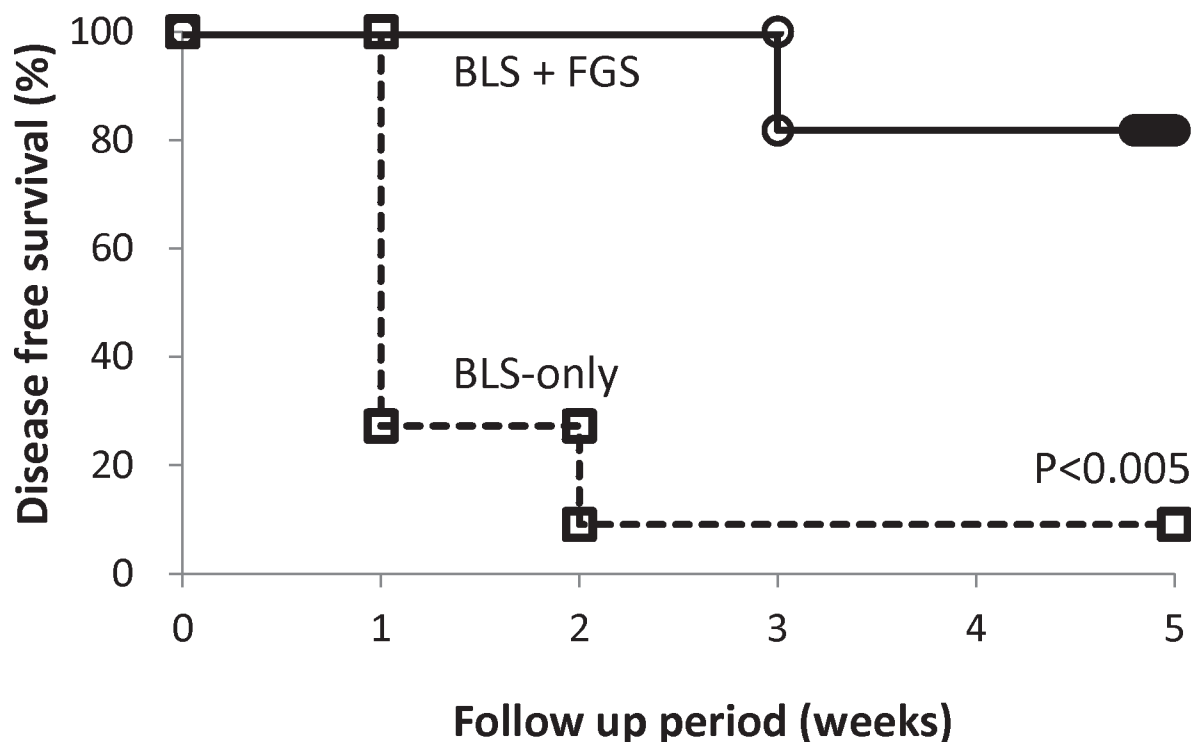


Figure 6. Kaplan-Meier curve for disease-free survival (DFS). Five-week DFS rates of BLS-only and BLS + FGS-treated mice were 9.1% and 81.8%, respectively. Mice treated with BLS + FGS had a significantly higher survival rate than mice treated with BLS-only ($p < 0.005$).

doi:10.1371/journal.pone.0116865.g006

Supporting Information

S1 ARRIVE Checklist
(PDF)

Acknowledgments

This paper is dedicated to the memory of A. R. Moossa, M.D.

Author Contributions

Conceived and designed the experiments: FU RMH. Performed the experiments: FU YH. Analyzed the data: FU YH SM YT SY MY YM HM KT MB FK RMH. Contributed reagents/materials/analysis tools: RMH. Wrote the paper: FY YT RMH.

References

1. Jaques DP, Coit DG, Hajdu SI, Brennan MF (1990) Management of primary and recurrent soft-tissue sarcoma of the retroperitoneum. *Ann Surg* 212:51–59. doi: [10.1097/0000658-199007000-00008](https://doi.org/10.1097/0000658-199007000-00008) PMID: [2363604](https://pubmed.ncbi.nlm.nih.gov/2363604/)
2. Karakousis CP, Gertenbluth R, Kontzoglou K, Driscoll DL (1995) Retroperitoneal sarcomas and their management. *Arch Surg* 130:1104–1109. doi: [10.1001/archsurg.1995.01430100082016](https://doi.org/10.1001/archsurg.1995.01430100082016) PMID: [7575124](https://pubmed.ncbi.nlm.nih.gov/7575124/)
3. Strauss DC, Hayes AJ, Thway K, Moskovic EC, Fisher C, et al. (2010) Surgical management of primary retroperitoneal sarcoma. *Br J Surg* 97:698–706. doi: [10.1002/bjs.6994](https://doi.org/10.1002/bjs.6994) PMID: [20306527](https://pubmed.ncbi.nlm.nih.gov/20306527/)
4. Lewis JJ, Leung D, Woodruff JM, Brennan MF (1998) Retroperitoneal soft-tissue sarcoma: analysis of 500 patients treated and followed at a single institution. *Ann Surg* 228:355–365. doi: [10.1097/0000658-199809000-00008](https://doi.org/10.1097/0000658-199809000-00008) PMID: [9742918](https://pubmed.ncbi.nlm.nih.gov/9742918/)

5. Bonvalot S, Rivoire M, Castaing M, Stoeckle E, Le Cesne A, et al. (2009) Primary retroperitoneal sarcomas: a multivariate analysis of surgical factors associated with local control. *J Clin Oncol* 27:31–37. doi: [10.1200/JCO.2008.18.0802](https://doi.org/10.1200/JCO.2008.18.0802) PMID: [19047280](https://pubmed.ncbi.nlm.nih.gov/19047280/)
6. Bouvet M, Hoffman RM (2011) Glowing tumors make for better detection and resection. *Sci Transl Med* 3:110fs10. doi: [10.1126/scitranslmed.3003375](https://doi.org/10.1126/scitranslmed.3003375) PMID: [22116932](https://pubmed.ncbi.nlm.nih.gov/22116932/)
7. Kishimoto H, Zhao M, Hayashi K, Urata Y, Tanaka N, et al. (2009) In vivo internal tumor illumination by telomerase-dependent adenoviral GFP for precise surgical navigation. *Proc Natl Acad Sci USA* 106:14514–14517. doi: [10.1073/pnas.0906388106](https://doi.org/10.1073/pnas.0906388106) PMID: [19706537](https://pubmed.ncbi.nlm.nih.gov/19706537/)
8. Kishimoto H, Urata Y, Tanaka N, Fujiwara T, Hoffman RM (2009) Selective metastatic tumor labeling with green fluorescent protein and killing by systemic administration of telomerase-dependent adenoviruses. *Mol Cancer Therap* 8:3001–3008. doi: [10.1158/1535-7163.MCT-09-0556](https://doi.org/10.1158/1535-7163.MCT-09-0556) PMID: [19887549](https://pubmed.ncbi.nlm.nih.gov/19887549/)
9. Kishimoto H, Aki R, Urata Y, Bouvet M, Momiyama M, et al. (2011) Tumor-selective adenoviral-mediated GFP genetic labeling of human cancer in the live mouse reports future recurrence after resection. *Cell Cycle* 10:2737–2741. doi: [10.4161/cc.10.16.16756](https://doi.org/10.4161/cc.10.16.16756) PMID: [21785265](https://pubmed.ncbi.nlm.nih.gov/21785265/)
10. Metildi CA, Kaushal S, Hardamon CR, Snyder CS, Pu M, et al. (2012) Fluorescence-guided surgery allows for more complete resection of pancreatic cancer, resulting in longer disease-free survival compared with standard surgery in orthotopic mouse models. *J Am Coll Surg* 215:126–136. doi: [10.1016/j.jamcollsurg.2012.02.021](https://doi.org/10.1016/j.jamcollsurg.2012.02.021) PMID: [22632917](https://pubmed.ncbi.nlm.nih.gov/22632917/)
11. Momiyama M, Kumamoto T, Suetsugu A, Kishimoto H, Chishima T, et al. (2012) Major liver resection stimulates stromal recruitment and metastasis compared with repeated minor resection. *J Surg Res* 178:280–287. doi: [10.1016/j.jss.2012.03.020](https://doi.org/10.1016/j.jss.2012.03.020) PMID: [22487397](https://pubmed.ncbi.nlm.nih.gov/22487397/)
12. Metildi CA, Kaushal S, Snyder CS, Hoffman RM, Bouvet M (2013) Fluorescence-guided surgery of human colon cancer increases complete resection resulting in cures in an orthotopic nude mouse model. *J Surg Res* 179:87–93. doi: [10.1016/j.jss.2012.08.052](https://doi.org/10.1016/j.jss.2012.08.052) PMID: [23079571](https://pubmed.ncbi.nlm.nih.gov/23079571/)
13. Momiyama M, Hiroshima Y, Suetsugu A, Tome Y, Mii S, et al. (2013) Enhanced resection of orthotopic red-fluorescent-protein-expressing human glioma by fluorescence-guided surgery in nude mice. *Anticancer Res* 33:107–112. PMID: [23267134](https://pubmed.ncbi.nlm.nih.gov/23267134/)
14. Hiroshima Y, Maawy A, Sato S, Murakami T, Uehara F, et al. (2014) Hand-held high-resolution fluorescence imaging system for fluorescence-guided surgery of patient and cell-line pancreatic tumors growing orthotopically in nude mice. *J Surg Res* 187:510–517. doi: [10.1016/j.jss.2013.11.1083](https://doi.org/10.1016/j.jss.2013.11.1083) PMID: [24373959](https://pubmed.ncbi.nlm.nih.gov/24373959/)
15. Hiroshima Y, Maawy A, Zhang Y, Sato S, Murakami T, et al. (2014) Fluorescence-guided surgery in combination with UVC irradiation cures metastatic human pancreatic cancer in orthotopic mouse models. *PLoS One* 9:e99977. doi: [10.1371/journal.pone.0099977](https://doi.org/10.1371/journal.pone.0099977) PMID: [24924955](https://pubmed.ncbi.nlm.nih.gov/24924955/)
16. Miwa S, Matsumoto Y, Hiroshima Y, Yano S, Uehara F, et al. (2014) Fluorescence-guided surgery of prostate cancer bone metastasis. *J Surg Res* 192:124–133. doi: [10.1016/j.jss.2014.05.049](https://doi.org/10.1016/j.jss.2014.05.049) PMID: [24972740](https://pubmed.ncbi.nlm.nih.gov/24972740/)
17. McElroy M, Kaushal S, Luiken G, Moossa AR, Hoffman RM, et al. (2008) Imaging of primary and metastatic pancreatic cancer using a fluorophore-conjugated anti-CA19-9 antibody for surgical navigation. *World J Surg* 32:1057–1066. doi: [10.1007/s00268-007-9452-1](https://doi.org/10.1007/s00268-007-9452-1) PMID: [18264829](https://pubmed.ncbi.nlm.nih.gov/18264829/)
18. Kaushal S, McElroy MK, Luiken GA, Talamini MA, Moossa AR, et al. (2008) Fluorophore-conjugated anti-CEA antibody for the intraoperative imaging of pancreatic and colorectal cancer. *J Gastrointest Surg* 12:1938–1950. doi: [10.1007/s11605-008-0581-0](https://doi.org/10.1007/s11605-008-0581-0) PMID: [18665430](https://pubmed.ncbi.nlm.nih.gov/18665430/)
19. Metildi CA, Kaushal S, Lee C, Hardamon CR, Snyder CS, et al. (2012) An LED light source and novel fluorophore combinations improve fluorescence laparoscopic detection of metastatic pancreatic cancer in orthotopic mouse models. *J Am Coll Surg* 214:997–1007. doi: [10.1016/j.jamcollsurg.2012.02.009](https://doi.org/10.1016/j.jamcollsurg.2012.02.009) PMID: [22542065](https://pubmed.ncbi.nlm.nih.gov/22542065/)
20. Wu J, Ma R, Cao H, Wang Z, Jing C, et al. (2013) Intraoperative imaging of metastatic lymph nodes using a fluorophore-conjugated antibody in a HER2/neu-expressing orthotopic breast cancer mouse model. *Anticancer Res* 33:419–424. PMID: [23393332](https://pubmed.ncbi.nlm.nih.gov/23393332/)
21. Maawy AA, Hiroshima Y, Kaushal S, Luiken GA, Hoffman RM, et al. (2013) Comparison of a chimeric anti-carcinoembryonic antigen antibody conjugated with visible or near-infrared fluorescent dyes for imaging pancreatic cancer in orthotopic nude mouse models. *J Biomed Optics* 18:126016. doi: [10.1117/1.JBO.18.12.126016](https://doi.org/10.1117/1.JBO.18.12.126016) PMID: [24356647](https://pubmed.ncbi.nlm.nih.gov/24356647/)
22. Metildi CA, Tang CM, Kaushal S, Leonard SY, Magistri P, et al. (2013) In vivo fluorescence imaging of gastrointestinal stromal tumors using fluorophore-conjugated anti-KIT antibody. *Ann Surg Oncol Suppl* 3:693–700. doi: [10.1245/s10434-013-3172-6](https://doi.org/10.1245/s10434-013-3172-6) PMID: [23943029](https://pubmed.ncbi.nlm.nih.gov/23943029/)
23. Metildi CA, Kaushal S, Pu M, Messer KA, Luiken GA, et al. (2014) Fluorescence-guided surgery with a fluorophore-conjugated antibody to carcinoembryonic antigen (CEA), that highlights the tumor,

- improves surgical resection and increases survival in orthotopic mouse models of human pancreatic cancer. *Ann Surg Oncol* 21:1405–1411. doi: [10.1245/s10434-014-3495-y](https://doi.org/10.1245/s10434-014-3495-y) PMID: [24499827](https://pubmed.ncbi.nlm.nih.gov/24499827/)
24. Metildi CA, Kaushal S, Luiken GA, Talamini MA, Hoffman RM, et al. (2014) Fluorescently-labeled chimeric anti-CEA antibody improves detection and resection of human colon cancer in a patient-derived orthotopic xenograft (PDOX) nude mouse model. *J Surg Oncol* 109:451–458. doi: [10.1002/jso.23507](https://doi.org/10.1002/jso.23507) PMID: [24249594](https://pubmed.ncbi.nlm.nih.gov/24249594/)
25. Hiroshima Y, Maawy A, Metildi CA, Zhang Y, Uehara F, et al. (2014) Successful fluorescence-guided surgery on human colon cancer patient-derived orthotopic xenograft mouse models using a fluorophore-conjugated anti-CEA antibody and a portable imaging system. *J Laparoendosc Adv Surg Tech A* 24:241–247. doi: [10.1089/lap.2013.0418](https://doi.org/10.1089/lap.2013.0418) PMID: [24494971](https://pubmed.ncbi.nlm.nih.gov/24494971/)
26. Metildi CA, Kaushal S, Luiken GA, Hoffman RM, Bouvet M (2014) Advantages of fluorescence-guided laparoscopic surgery of pancreatic cancer labeled with fluorescent anti-carcinoembryonic antigen antibodies in an orthotopic mouse model. *J Am Coll Surg* 219:132–141. doi: [10.1016/j.jamcollsurg.2014.02.021](https://doi.org/10.1016/j.jamcollsurg.2014.02.021) PMID: [24768506](https://pubmed.ncbi.nlm.nih.gov/24768506/)
27. Maawy A, Hiroshima Y, Zhang Y, Luiken GA, Hoffman RM, et al. (2014) Polyethylene glycol (PEG) conjugations of chimeric anti-carcinoembryonic antigen (CEA) labeled with near infrared (NIR) dyes enhances imaging of liver metastases in a nude-mouse model of human colon cancer. *PLoS One* 9: e97965. doi: [10.1371/journal.pone.0097965](https://doi.org/10.1371/journal.pone.0097965) PMID: [24859320](https://pubmed.ncbi.nlm.nih.gov/24859320/)
28. Maawy A, Hiroshima Y, Zhang Y, Luiken GA, Hoffman RM, et al. (2014) Specific tumor labeling enhanced by polyethylene glycol linkage of near infrared dyes conjugated to a chimeric anti-carcinoembryonic antigen antibody in a nude mouse model of human pancreatic cancer. *J Biomed Optics* 19:101504. doi: [10.1117/1.JBO.19.10.101504](https://doi.org/10.1117/1.JBO.19.10.101504) PMID: [24887695](https://pubmed.ncbi.nlm.nih.gov/24887695/)
29. Metildi CA, Kaushal S, Luiken GA, Hoffman RM, Bouvet M (2014) Advantages of fluorescence-guided laparoscopic surgery of pancreatic cancer labeled with fluorescent anti-carcinoembryonic antigen antibodies in an orthotopic mouse model. *J Am Coll Surg* 219:132–141. doi: [10.1016/j.jamcollsurg.2014.02.021](https://doi.org/10.1016/j.jamcollsurg.2014.02.021) PMID: [24768506](https://pubmed.ncbi.nlm.nih.gov/24768506/)
30. Hiroshima Y, Maawy A, Sato S, Murakami T, Uehara F, et al. (2014) Hand-held high-resolution fluorescence imaging system for fluorescence-guided surgery of patient and cell-line pancreatic tumors growing orthotopically in nude mice. *J Surg Res* 187:510–517. doi: [10.1016/j.jss.2013.11.1083](https://doi.org/10.1016/j.jss.2013.11.1083) PMID: [24373959](https://pubmed.ncbi.nlm.nih.gov/24373959/)
31. Yamamoto N, Yang M, Jiang P, Tsuchiya H, Tomita K, et al. (2003) Real-time GFP imaging of spontaneous HT-1080 fibrosarcoma lung metastases. *Clin Exp Metastasis* 20:181–185. doi: [10.1023/A:1022662927574](https://doi.org/10.1023/A:1022662927574) PMID: [12705639](https://pubmed.ncbi.nlm.nih.gov/12705639/)
32. Yamamoto N, Yang M, Jiang P, Xu M, Tsuchiya H, et al. (2003) Determination of clonality of metastasis by cell-specific color-coded fluorescent-protein imaging. *Cancer Res* 63:7785–7790. PMID: [14633704](https://pubmed.ncbi.nlm.nih.gov/14633704/)
33. Hoffman RM, Yang M (2006) Subcellular imaging in the live mouse. *Nature Protoc* 1:775–782. doi: [10.1038/nprot.2006.109](https://doi.org/10.1038/nprot.2006.109) PMID: [17406307](https://pubmed.ncbi.nlm.nih.gov/17406307/)
34. Hoffman RM, Yang M (2006) Color-coded fluorescence imaging of tumor-host interactions. *Nature Protoc* 1:928–935. doi: [10.1038/nprot.2006.119](https://doi.org/10.1038/nprot.2006.119) PMID: [17406326](https://pubmed.ncbi.nlm.nih.gov/17406326/)
35. Hoffman RM, Yang M (2006) Whole-body imaging with fluorescent proteins. *Nature Protoc* 1:1429–1438. doi: [10.1038/nprot.2006.223](https://doi.org/10.1038/nprot.2006.223) PMID: [17406431](https://pubmed.ncbi.nlm.nih.gov/17406431/)
36. Yamauchi K, Yang M, Jiang P, Xu M, Yamamoto N, et al. (2006) Development of real-time subcellular dynamic multicolor imaging of cancer-cell trafficking in live mice with a variable-magnification whole-mouse imaging system. *Cancer Res* 66:4208–4214. doi: [10.1158/0008-5472.CAN-05-3927](https://doi.org/10.1158/0008-5472.CAN-05-3927) PMID: [16618743](https://pubmed.ncbi.nlm.nih.gov/16618743/)
37. Kimura H, Momiyama M, Tomita K, Tsuchiya H, Hoffman RM (2010) Long-working-distance fluorescence microscope with high-numerical-aperture objectives for variable-magnification imaging in live mice from macro- to subcellular. *J Biomed Optics* 15:066029. doi: [10.1117/1.3526356](https://doi.org/10.1117/1.3526356) PMID: [21198203](https://pubmed.ncbi.nlm.nih.gov/21198203/)
38. Hiroshima Y, Maawy A, Zhang Y, Sato S, Murakami T, et al. (2014) Fluorescence-guided surgery in combination with UVC irradiation cures metastatic human pancreatic cancer in orthotopic mouse models. *PLoS One* 9:e99977. doi: [10.1371/journal.pone.0099977](https://doi.org/10.1371/journal.pone.0099977) PMID: [24924955](https://pubmed.ncbi.nlm.nih.gov/24924955/)
39. Kimura H, Zhang L, Zhao M, Hayashi K, Tsuchiya H, et al. (2010) Targeted therapy of spinal cord glioma with a genetically-modified *Salmonella typhimurium*. *Cell Prolif* 43:41–48. doi: [10.1111/j.1365-2184.2009.00652.x](https://doi.org/10.1111/j.1365-2184.2009.00652.x) PMID: [19922490](https://pubmed.ncbi.nlm.nih.gov/19922490/)
40. Miwa S, Yano S, Zhang Y, Matsumoto Y, Uehara F, et al. (2014) Tumor-targeting *Salmonella typhimurium* A1-R prevents experimental human breast cancer bone metastasis in nude mice. *Oncotarget* 5:7119–7125. PMID: [25216526](https://pubmed.ncbi.nlm.nih.gov/25216526/)

41. Kimura H, Lee C, Hayashi K, Yamauchi K, Yamamoto N, et al. (2010) UV light killing efficacy of fluorescent protein-expressing cancer cells in vitro and in vivo. *J Cell Biochem* 110:1439–1446. doi: [10.1002/jcb.22693](https://doi.org/10.1002/jcb.22693) PMID: [20506255](https://pubmed.ncbi.nlm.nih.gov/20506255/)
42. Glinsky GV (2013) RNA-guided diagnostics and therapeutics for next-generation individualized nanomedicine. *J Clin Invest* 123:2350–2352 doi: [10.1172/JCI69268](https://doi.org/10.1172/JCI69268) PMID: [23728168](https://pubmed.ncbi.nlm.nih.gov/23728168/)